



ARTICLE

The Study on Bamboo Microfibers Isolated by Steam Explosion and Their Comprehensive Properties

Qiushi Li^{1,2,#}, Ronggang Luo^{1,2,#}, Yu Chen³, Jinhui Xiong³, Bei Qiao¹, Xijuan Chai^{1,2}, Linkun Xie^{1,2}, Juan Wang³, Lianpeng Zhang^{1,2,*}, Siqun Wang⁴, Guanben Du^{1,2} and Kaimeng Xu^{1,2,*}

¹Yunnan Provincial Key Laboratory of Wood Adhesives and Glued Products, Southwest Forestry University, Kunming, 650224, China

²International Joint Research Center for Biomass Materials, Ministry of Science and Technology, Southwest Forestry University, Kunming, 650224, China

³Key Laboratory for Forestry Resources Conversion and Utilization in the Southwest Mountains of China, Ministry of Education, Southwest Forestry University, Kunming, 650224, China

⁴Center for Renewable Carbon, The University of Tennessee, Knoxville, TN, 37996, USA

*Corresponding Authors: Kaimeng Xu. Email: xukm007@163.com; Lianpeng Zhang. Email: lpz@zju.edu.cn

#Qiushi Li and Ronggang Luo contributed equally to this work

Received: 22 August 2022 Accepted: 11 October 2022

ABSTRACT

To overcome the shortage of wood resources as well as to develop novel natural fibers materials, the *Chimonobambusa quadrangularis* (CQ) and *Qiongzhusua tumidinoda* (QT) planted in Southwest China were effectively isolated by the steam explosion (SE). The fine and uniform bamboo microfibers derived from CQ and QT were obtained, and their smallest average widths were 12.62 μm and 16.05 μm , respectively. The effects of steam explosion on the micro-morphology, chemical composition, thermal stability, crystallinity, surface wettability, and mechanical properties of bamboo microfibers were comprehensively investigated. The results showed that the relative content of cellulose in bamboo microfibers increased but the hemicellulose and lignin contents decreased after SE. The degrees of crystallinity for CQ and QT increased from 40.49% and 39.46% to 68.90% and 55.78%, respectively. The thermal stability and surface hydrophilicity were also improved. The CQ microfibers had a maximum decomposition temperature of 2.79°C, a tensile strength of 58.54 MPa, an elongation at break of 0.6%, and a water contact angle of 2.7° higher than those of the QT microfibers.

KEYWORDS

Microfiber properties; bamboo; steam explosion; *Chimonobambusa quadrangularis*; *Qiongzhusua tumidinoda*

1 Introduction

With the shortage of wood resources worldwide, the demand for renewable biomass resources for industrial production is rapidly increasing. Bamboo is one of the most important and fastest-growing non-woody biomass resources in the world with more than 1600 species [1]. There are over 500 bamboo species and more than 30 million hm^2 forest area in China [2,3]. *Chimonobambusa quadrangularis* (CQ) and *Qiongzhusua tumidinoda* (QT) are two distinctive bamboo species in Southwest of China. Natural



bamboo resources with the advantages of high productivity, rapid growth rate, easy propagation, and excellent mechanical properties have been widely used in handicrafts, paper and textile industry, as well as building and construction [4,5]. In recent years, bamboo fibers with high cellulose contents have been paid more attention in several advanced applications including natural fiber-reinforced polymer composites, adsorption, electromagnetic shielding, and storage-energy functional materials [6]. They are usually isolated by various physical or chemical methods [7,8]. Steam explosion (SE) is an eco-friendly isolation technology with low energy consumption and a facile process [9–12].

The bamboo microfibers of *Bambusa beecheyama* with an average width of $16.7 \pm 4.8 \mu\text{m}$ were successfully prepared using SE. The average widths of bamboo microfibers can be further decreased to $7.5 \pm 3.2 \mu\text{m}$ with a combination of alkaline and bleaching treatments [13]. Boonterm et al. comparatively studied the difference between isolated fibers by chemical treatment and SE treatment. The latter can break down the natural fibers more effectively with the smaller average widths and the larger aspect ratio, also had a higher fiber yield in comparison with the former [14]. The various biomass microfibers from wood, rice straw, kenaf, and pineapple leaf also have been successfully isolated by SE with a similar effect to the traditional alkaline treatment [15].

Chimonobambusa quadrangularis with a square-shaped culm is known as “Square Bamboo”, which is widely planted in Yunnan Province, China [16]. *Qiongzhueta tumidinoda*, only planted in Sichuan and Yunnan Provinces, is a kind of fast-growing bamboo species with a peculiar-shaped culm [17]. It is crucial to understand the physical properties and chemical composition of various bamboo raw materials due to their inherent complexity and variability [18]. To address the increasing interests in novel natural bamboo fiber functional materials and expand its application across various fields, this study aims to develop a facile, low-cost, and environmental-friendly way to prepare bamboo microfibers from CQ and QT via SE. The optimal technology parameters of SE for two bamboo species were investigated by the orthogonal experiment. The variations in the micro-morphology, chemical composition, thermal stability, crystallinity, surface wettability, and mechanical properties of bamboo microfibers after SE were characterized by the scanning electron microscopy (SEM), Fourier transform infrared spectroscopy (FTIR), thermogravimetric analysis (TGA), X-ray diffraction (XRD), water contact angle measurement (WCA), and electronic mechanical instrument. The main chemical compositions of the bamboo samples before and after SE were also analyzed according to the National Renewable Energy Laboratory (NREL) standard.

2 Materials and Methods

2.1 Materials

The *Chimonobambusa quadrangularis* and *Qiongzhueta tumidinoda* were harvested in Dagan County, Yunnan Province, Southwest of China. Three-year-old bamboos were chosen without insect pests and physical defects. The bamboo culms were cut into small strips with dimensions of $60 \text{ mm} \times 10 \text{ mm} \times 10 \text{ mm}$ in length, width, and thickness. Then they were air-dried for one month.

2.2 Orthogonal Experiment of Steam Explosion

An orthogonal experiment of steam explosion with X (soaking time), Y (pressure of SE), and Z (residence time) as factors corresponding to three levels was carried out according to Table 1 on a steam explosion instrument (QBS-80, Gentle Bioenergy (Hebei) Co. Ltd., China). About 25 g of bamboo strips were soaked and then placed in a 0.4 L steam blast chamber. The saturated steam flowed into the chamber to increase the pressure of the chamber. Subsequently, the steam pressure was immediately released when the setting parameters were obtained.

2.3 Characterization and Measurement

2.3.1 Optical Microscopy Analysis

The width and distribution of bamboo microfibers after SE were examined using an LED light microscope (DM2000, Leica, Germany) equipped with a camera (DMC 4500, Leica, Germany).

Table 1: The orthogonal experiment of steam explosion for the bamboo

Group codes	Soaking time (h)	Pressure (MPa)	Residence time (s)
A	12	1.7	250
B	12	2.0	350
C	12	2.3	300
D	24	1.7	350
E	24	2.0	300
F	24	2.3	250
G	36	1.7	300
H	36	2.0	250
I	36	2.3	350

2.3.2 Scanning Electron Micrograph (SEM) Observation

The SEM (Zeiss Sigma VP, Germany) was used for the micromorphological analysis of the steam-exploded samples with gold coating at an accelerating voltage of 5 kV.

2.3.3 Fourier Transfer Infrared Spectroscopy (FTIR) Analysis

FTIR spectra of the bamboos before and after SE were measured on a Nicolet IS5 spectrometer (Waltham, MA, USA) with the potassium bromide pellet way. The scanning frequency was 32 times in the wave number range of 4000~400 cm^{-1} .

2.3.4 Thermogravimetric (TGA) Analysis

The thermogravimetric curves of the bamboos before and after SE were tested by a thermogravimetric instrument (TG209-F1, Netzsch, Germany). About 5–10 mg specimens were heated to 800°C with a heating rate of 10 °C/min under a nitrogen atmosphere.

2.3.5 The Main Chemical Composition Analysis

The main chemical compositions were measured according to the standard “Determination of Structural Carbohydrates and Lignin in Biomass” issued by the National Renewable Energy Laboratory (NREL).

2.3.6 X-ray Diffraction (XRD) Analysis

XRD measurements of the bamboos before and after SE were carried out on a diffractometer (Ultima IV, Rigaku, Japan) using Cu- α as the X-ray source ($\lambda = 0.15406$ nm) at a 40 kV accelerating voltage. The rotational range of the diffraction angle, the scanning speed, and the incremental step were 10°–60°, 2°/min, and 0.02°, respectively. The degree of crystallinity for cellulose can be calculated by Eq. (1).

$$CrI(\%) = \frac{I_{002} - I_{am}}{I_{002}} \times 100 \quad (1)$$

where I_{002} is the peak intensity of the (002) lattice diffraction at $2\theta = 22.6^\circ$, representing the crystalline and amorphous region of cellulose, and I_{am} is the diffraction intensity of amorphous fraction at $2\theta = 18^\circ$.

2.3.7 Water Contact Angle (WCA) Measurement

WCA measurements of the bamboo microfibers were performed on a JC2000D3R contact angle instrument (Shanghai Zhongchen Digital Technology Equipment Co., Ltd., China) at ambient temperature. Two microliters of distilled water were dropped onto the surface of the specimens. The average WCA values were calculated from the data at three different positions on each sample.

2.3.8 The Test of Mechanical Properties

An electronic mechanical instrument (5583, Instron, USA) was used to test the mechanical properties of the bamboo microfibers. The samples with 50 mm length were placed between two grips with a 20 mm gauge length and were tested at a 1 mm/min crosshead speed.

3 Results and Discussion

3.1 The Width Distribution of Bamboo Microfibers

The main SE process chart for the bamboo is shown in Fig. 1. The appearance and width distribution of bamboo microfibers after SE for CQ and QT are presented in Figs. 2 and 3. It is seen that the bamboo microfibers were successfully obtained by SE with various colors and width sizes, which can be explained by the difference in the major chemical composition and anatomical structure of two bamboo species. The significant factors on CQ microfibers in orthogonal experiments of SE were ranked as X (soaking time) > Y (pressure) > Z (residence time) according to the range and variance analysis. The smallest average width for CQ was 81.82 μm . Similarly, as for QT, the significant factors in orthogonal experiments of SE were ranked as Y (pressure) > X (soaking time) > Z (residence time). The smallest value of average width was 71.32 μm . There was a little difference in the microfiber size for both bamboo species. To obtain the finest bamboo microfibers, the optimal parameters of SE for CQ and QT were $X_1Y_3Z_3$ (12 h, 2.3 MPa, 350 s) and $X_1Y_2Z_2$ (12 h, 2.0 MPa, 300 s), respectively.

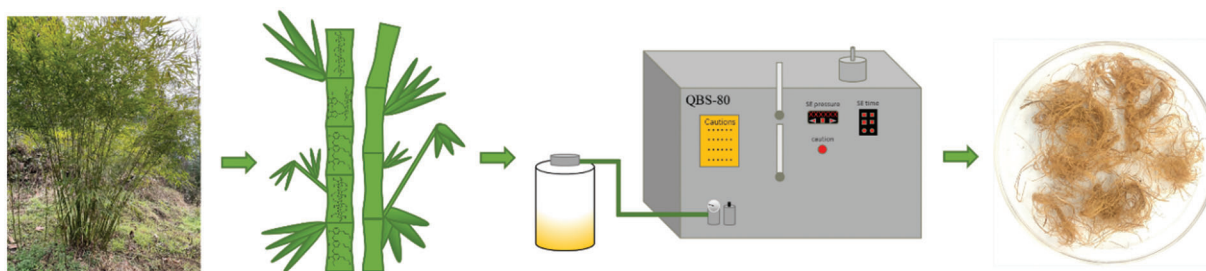


Figure 1: The chart of bamboo microfiber preparation by SE

3.2 SEM Observation

The micro morphology of the bamboo culms and isolated bamboo microfibers are displayed in Fig. 4. The cross-section of the bamboo culms appeared with many intact vascular bundles consisting of hollow vessels surrounded by fibrous sclerenchyma cells before SE [19]. It is observed that CQ had thicker and smaller vessels than those of QT, as shown in Figs. 4a and 4d. The average thickness values and diameters of vessels for CQ and QT were $2.86 \pm 0.09 \mu\text{m}$, $7.02 \pm 0.35 \mu\text{m}$ and $1.24 \pm 0.02 \mu\text{m}$, $45.71 \pm 1.26 \mu\text{m}$, respectively. The long bamboo microfibers were effectively isolated when subjected to rapid depressurization and shearing during SE, as seen in Figs. 4b, 4c and 4e, 4f. The bamboo microfibers generally were uniform in width, with average widths of $12.62 \pm 1.79 \mu\text{m}$ and $16.05 \pm 2.18 \mu\text{m}$, which implied that the thicker cell walls and smaller diameters of bamboos with more fibrous tissues had higher shearing at the sudden release of pressure and thus facilitated the rupture of glycosidic bond and hydrogen bonds of cellulose as well as the subsequent hydrolysis of hemicellulose [20]. Residual hemicellulose and lignin that acted as binders were not found on the surface after the SE process, which was due to the washing process by deionized water prior to SEM observation [21]. The fibrous structures provide the bamboos with great application prospects in some novel functional materials including fiber-reinforced polymer composites, adsorption, purification, storage-energy, and sensing materials of porous biomass fibrous mats or sheets.

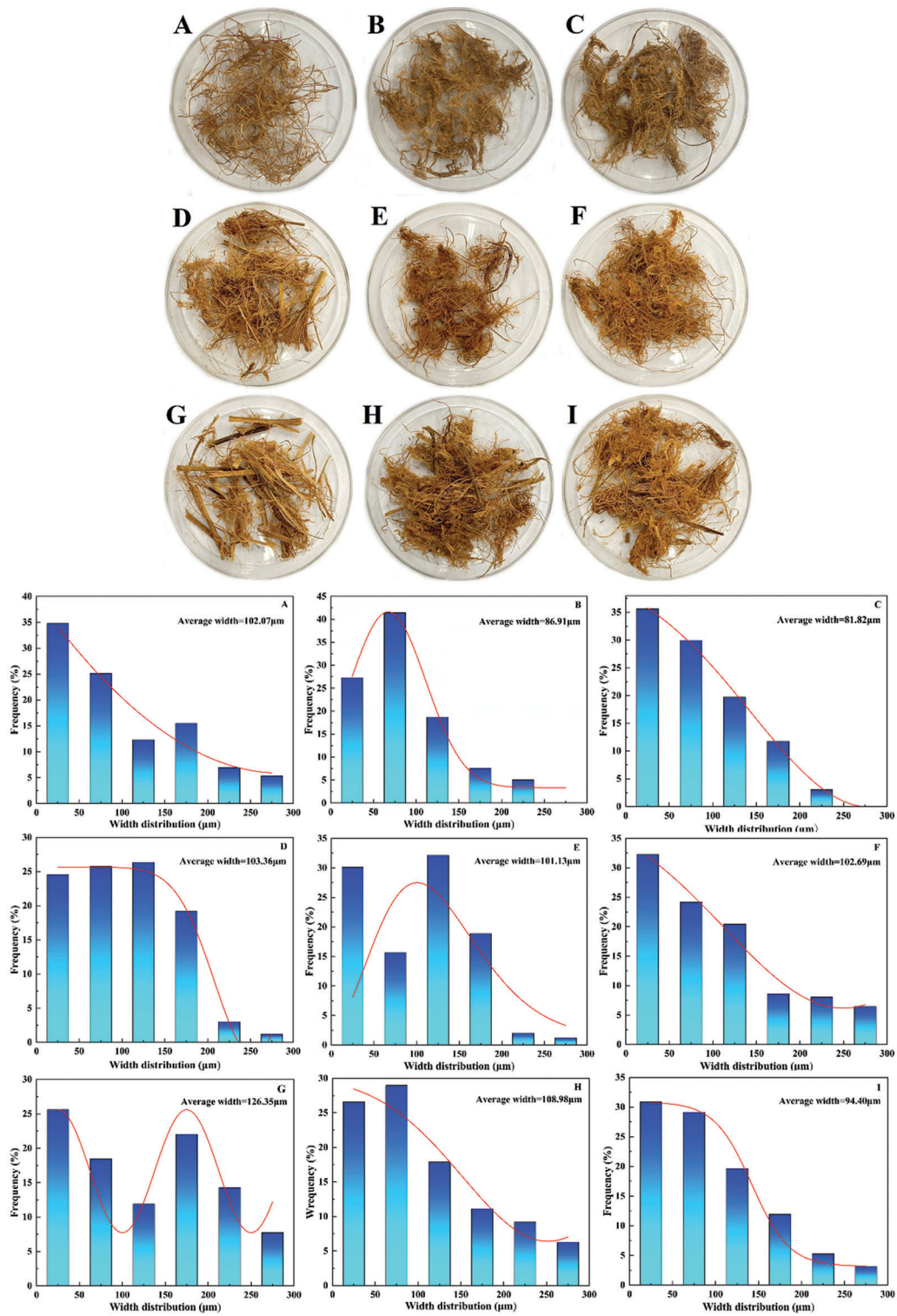


Figure 2: The average width and distribution of bamboo microfibers after SE for CQ

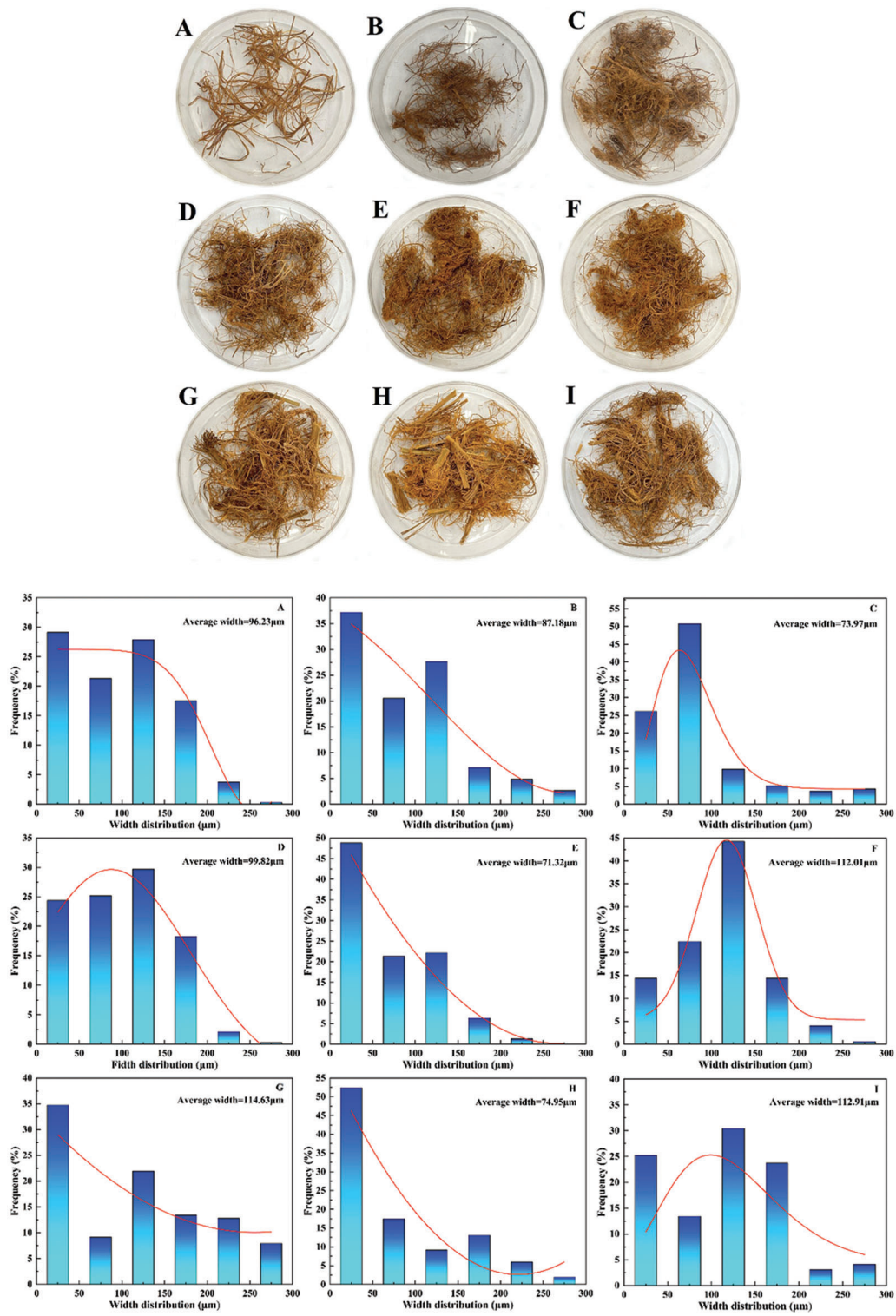


Figure 3: The average width and distribution of bamboo microfibers after SE for QT

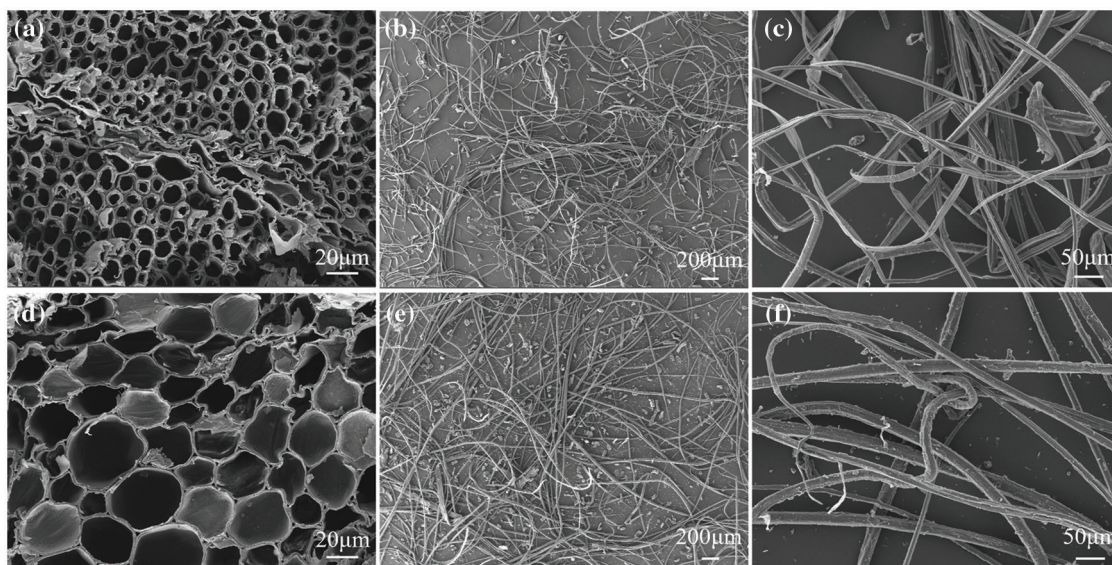


Figure 4: The SEM images of the bamboos before and after SE: (a) CQ control; (b) CQ SE; (c) CQ SE; (d) QT control; (e) QT SE; (f) QT SE

3.3 Analysis of FTIR

The FTIR spectra of the two bamboo species before and after SE are shown in Fig. 5. All the bamboo samples including culms and microfibers appeared the similar curves, which meant that they had the similar main chemical compositions [22]. The broad absorption bands from 3000 to 3800 cm^{-1} are associated with the stretching vibrations of the $-\text{OH}$ groups in the cellulose, hemicellulose, lignin as well as the absorbing water [23]. A small band at 2920 cm^{-1} is related to the stretching vibration of $\text{C}-\text{H}$ in cellulose and hemicellulose [24]. The peak at around 1730 cm^{-1} may correspond to the acetyl and uronic ester of hemicellulose as well as the carboxylic groups of ferulic and *p*-coumaric acid in lignin and hemicellulose [25]. The adsorption bands located at 1512 , 1378 , and 1254 cm^{-1} are assigned to the aromatic ring vibration of lignin. The band at 1050 cm^{-1} corresponds to the stretching vibration of $\text{C}-\text{O}-\text{C}$ for the glycosidic bonds and the pyranose ring in the molecular chains of cellulose [26]. It is noted that the intensities of the adsorption bands at 3435 , 2929 , 1040 , 1378 , and 1254 cm^{-1} increased when bamboo culms were subjected to SE, inferring that more cellulose and lignin were generated. This can be explained as monomeric sugars and oligomeric were formed with partially soluble and decomposed small molecular substances like furfural due to the auto-hydrolysis of hemicellulose [27]. Ester bonds in carbohydrates and lignin were broken down during SE [28], which resulted in the melting and recondensation of lignin possibly covering on the surface of bamboo microfibers.

3.4 Analysis of the Main Chemical Composition

The chemical composition variation of the bamboo samples before and after SE is illustrated in Fig. 6. The bamboo culms for both species showed moderate contents of hemicellulose and lignin and a high content of cellulose before SE treatment [29]. The three main chemical components (cellulose, hemicellulose, and lignin) for the CQ control and the QT control were $46.29\% \pm 0.20\%$, $23.20\% \pm 0.11\%$, and $30.51\% \pm 0.06\%$ and $45.80\% \pm 0.09\%$, $22.82\% \pm 0.17\%$, and $31.38\% \pm 0.14\%$, respectively. According to previous reports, the general contents of cellulose, hemicellulose and lignin for most lignocellulosic biomasses are 25–45, 20–40, and 10–25 wt%, respectively, while for bamboo is typically 42–47 wt% for cellulose, 22–24 wt% for hemicellulose, and 23–31 wt% for lignin [30]. This implied that CQ and QT were two outstanding raw materials for the development of novel natural microfiber materials. The relative content

of cellulose in bamboo microfibrils showed a marked increase from $46.29\% \pm 0.20\%$ to $58.03\% \pm 0.13\%$ for CQ and $45.80\% \pm 0.09\%$ to $54.00\% \pm 0.11\%$ for QT after SE. However, the hemicellulose content decreased from $23.20\% \pm 0.11\%$ and $22.82\% \pm 0.17\%$ to $14.16\% \pm 0.06\%$ and $18.74\% \pm 0.15\%$ for CQ and QT, respectively. There was a slight reduction in lignin content from $30.51\% \pm 0.06\%$ to $27.81\% \pm 0.19\%$ for CQ and $31.38\% \pm 0.14\%$ to $27.25\% \pm 0.13\%$ for QT, respectively. During the SE process, hemicellulose was auto-hydrolyzed by acetic acid, lignin was depolymerized and recondensed, and the amorphous cellulose was disrupted. The fibrous structures were formed by the combined effects of water flushing, volume expansion, and tissue isolation, resulting in variation of the main chemical composition and redistribution of partial components.

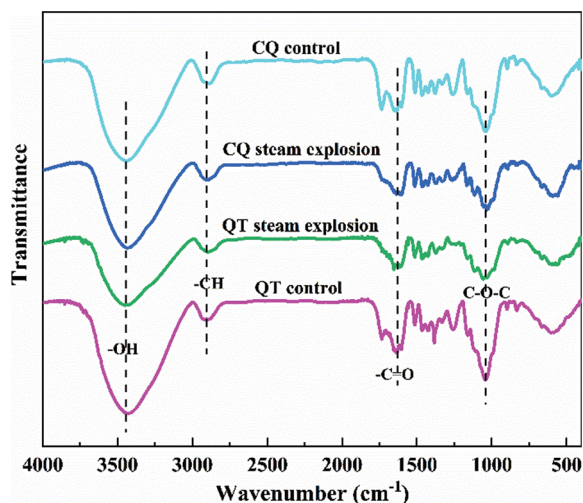


Figure 5: The FTIR spectra of the bamboos before and after SE

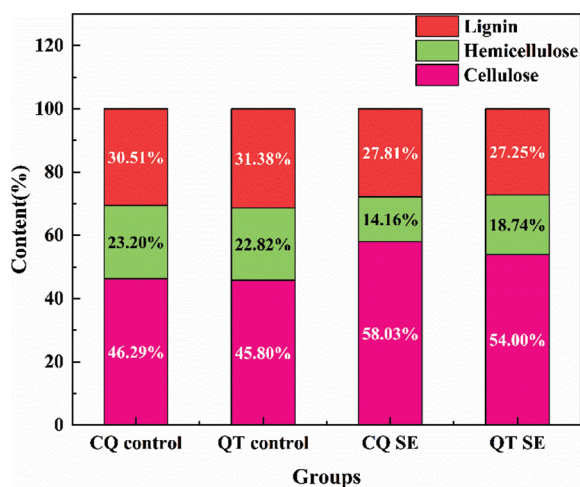


Figure 6: The variation of the main chemical composition of the bamboos before and after SE

3.5 Thermal Stability Analysis

Fig. 7 displays the thermogravimetric (TG) and derivative thermogravimetric (DTG) curves for CQ and QT before and after SE at the optimum process parameters. Generally, there were three major stages of thermal decomposition for the bamboo specimens [31]. The first stage below 100°C corresponding to a

3%–5% mass loss was likely attributed to residual moisture evaporation. The main thermal decomposition was in the range of 190°C–450°C due to the cleavage of glycosidic linkages in cellulose, the rearrangement and cracking of cellulose, and the decarboxylation and decarbonylation of residual hemicellulose and partial lignin. The third stage across a broad temperature range (490°C–800°C) was mainly associated with the cleavage and fragmentation of the monomeric phenol units in lignin, yielding phenolic compounds, methanol, methane as well as CO₂, CO, and H₂O [32,33]. The maximum decomposition temperature (T_{\max}) corresponding to the maximum weight loss rate of the bamboo samples is displayed in Fig. 7b. There were remarkably elevated T_{\max} values for CQ and QT after SE treatment compared to their control samples. This can be explained that the removal and conversion of the hemicellulose and the relatively higher cellulose contents with a high molecular weight and an ordered arrangement delayed the thermal decomposition of bamboo microfibrils [33,34]. This is consistent with the analysis of the main chemical composition. The specific T_{\max} values increased from 341.32°C and 313.78°C to 366.43°C and 363.64°C, respectively, corresponding to the rates of increase of 7.36% and 15.89%, respectively [35], indicating that the thermal stability of CQ microfibrils was superior to that of QT.

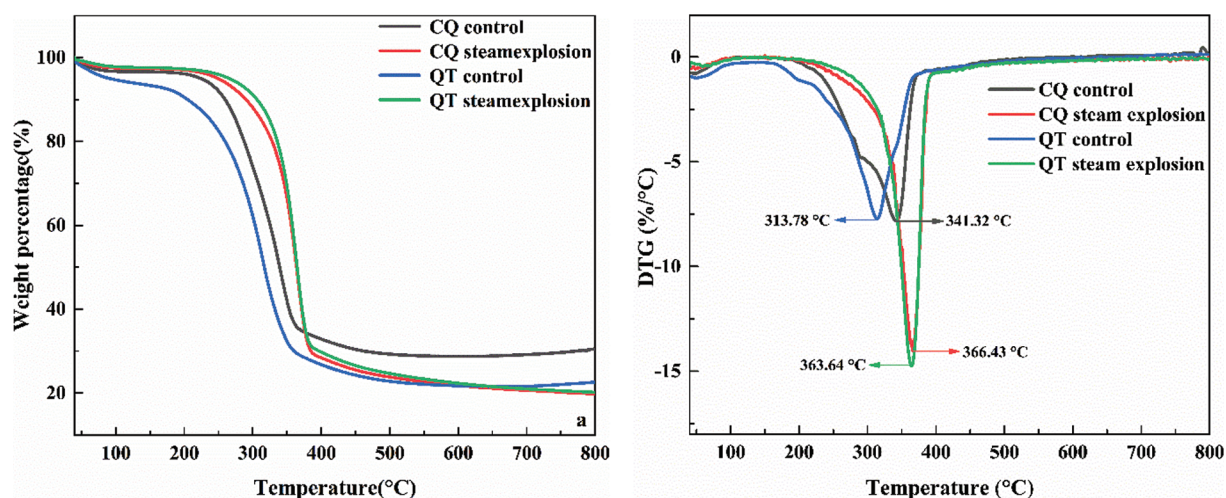


Figure 7: The TG and DTG curves of bamboo before and after SE

3.6 XRD Analysis

Fig. 8 shows the XRD profiles of the bamboos before and after SE. The characteristic peaks corresponding to $2\theta = 15.8^\circ$, 22.6° , and 34.5° are related to the (110), (002) and (040) crystalline planes, respectively [36]. The peaks for all bamboo samples were verified as the diffraction peaks of the cellulose I structure [37], which implied that SE treatment would not change the crystalline structure of cellulose. This is consistent with previous reports on other biomass resources. The sharper peak at 22.2° was due to the increase of crystallinity with the efficient removal of noncellulosic polysaccharides and the solvation of amorphous zones after SE treatment [38]. The degrees of crystallinity for CQ and QT were $40.49\% \pm 0.33\%$ and $39.46\% \pm 0.18\%$, respectively. Whereas they increased to $68.9\% \pm 0.25\%$ and $55.78\% \pm 0.11\%$ after SE treatment. This was due to the high temperature steam restructuring the amorphous and crystalline cellulose regions [39]. The strains that arise from the crystallization phase in the biosynthesis of native cellulose as well as the cell wall formation by cellulose interacting with hemicellulose and lignin were effectively released. In addition, the weak peaks at 34.5° had a slight increase due to the exposure of crystalline cellulose on the surface of bamboo microfibrils after SE [40,41].

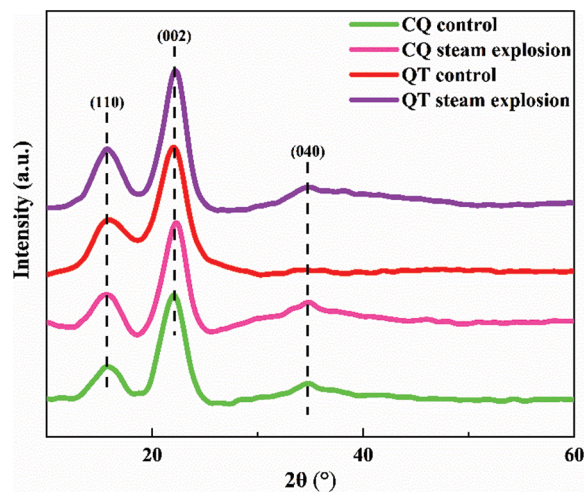


Figure 8: The XRD curves of bamboo before and after SE

3.7 CA Analysis

WCA measurements for bamboo microfibers were carried out using a sessile drop method on the compressed flat surface of microfibers [42]. As shown in Fig. 9, the images of water droplets clearly displayed the variations in surface wettability of two bamboo species. It can be noticed that there was an obvious difference in the control samples of CQ and QT. The former had a higher water contact angle value (101.5°) than that of the latter (96.25°), corresponding to the weaker hydrophilicity [43]. However, the hydrophilicity greatly increased when the bamboo culms were treated by SE and the corresponding WCA values were reduced to 83.2° and 80.5° , respectively [44]. The bamboo prior to SE had a chemically and physically integrated structure in which the hydrophilic cellulose was bound by hydrophobic lignin. However, the softening, partial degradation, redistribution, recondensation, and reshaping of the lignin components occurred after SE, leading to the exposure of more cellulose. Additionally, the inorganic impurities, such as silicon, in bamboo probably were reduced after SE treatment [45]. These results indicated that the SE treatment had a positive effect on the increase of the hydrophilicity on the bamboo surface. This is consistent with the analyses of chemical composition and FTIR [46].

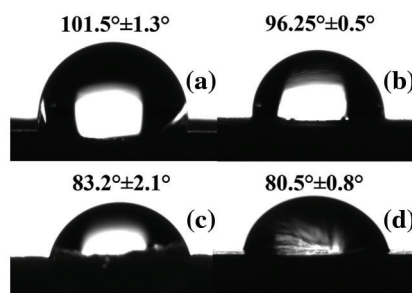


Figure 9: The water contact angles of bamboo before and after SE: (a) CQ control; (b) QT control; (c) CQ steam explosion; (d) QT steam explosion

3.8 The Analysis of Mechanical Properties

The mechanical properties of bamboo microfibers after SE are presented in Fig. 10. The cellulose fibers in bamboo species are made up of many cellulose molecules in an extended chain conformation, resulting in outstanding mechanical strength [47], which is also the crucial prerequisite for the functional application of

bamboo microfibers. The mechanical properties generally are determined by the chemical composition, the microfibrillar angles and the special layered structure of fiber cell walls [48]. The microfibers derived from CQ displayed a higher tensile strength (476.55 MPa) and elongation at break (5.3%) than those derived from QT after SE treatment. This was possibly due to the thick cell walls, the low hemicellulose content and the high microfibrillar angle in CQ microfibers effectively promoting their mechanical properties. Additionally, the weak interfacial bonding between the broad and narrow lamellae also facilitated the slipping of microfiber cell structures during tension. This is consistent with previous reports [49,50].

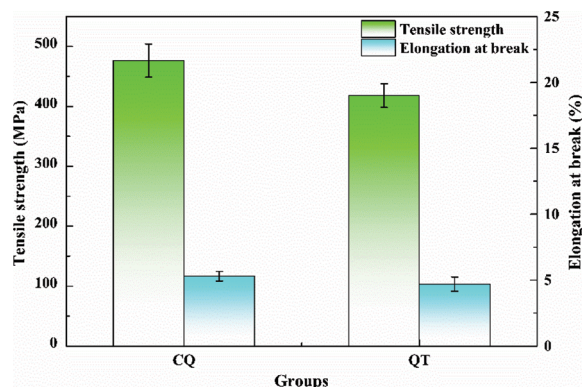


Figure 10: The mechanical properties of bamboo microfibers after SE

4 Conclusion

The fine and uniform bamboo microfibers derived from the CQ and QT planted in the Southwest of China were successfully isolated by steam explosion. The optimal parameters for the bamboo microfibers by the steam explosion were the soaking time of 12 h, the vapor pressure of 2.3 MPa, the residence time of 350 s for CQ and the soaking time of 12 h, the vapor pressure of 2.0 MPa and residence time of 300 s for QT, respectively. The two bamboo species had moderate contents of hemicellulose and lignin and a high content of cellulose. The relative content of cellulose in bamboos had a marked increase after SE treatment but a decrease for hemicellulose and lignin. The SE also improved the thermal stability, crystallinity, and surface hydrophilic properties of the bamboos. The degrees of crystallinity for CQ and QT increased from 40.49% and 39.46% to 68.90% and 55.78%, respectively. The CQ microfibers had a T_{max} of 2.79°C, a tensile strength of 58.54 MPa, an elongation at break of 0.6% and a water contact angle of 2.7° higher than those of the QT microfibers. Both bamboo species are excellent raw materials for the development of novel functional natural fiber materials in the future.

Acknowledgement: We sincerely appreciated the technical guidance by Professor Siqun Wang and Associate Professor Lianpeng Zhang, the supply of bamboo raw materials by Professor Juan Wang as well as the financial support by Professor Kaimeng Xu.

Funding Statement: This study was financially supported by the National Natural Science Foundation of China (NSFC) (32060381), the Applied Basic Research Programs of Yunnan Province (202201AT070058), the Scientific Research Funds of Educational Committee of Yunnan Province (2022Y552), the Opening Project of Guangxi Key Laboratory of Forest Products Chemistry and Engineering, China (GXFK2209), the High Level Innovative One-Ten-Thousand Youth Talents of Yunnan Province (YNWR-QNBJ-2020-203), the National College Students Innovation and Entrepreneurship Training Program (202110677009), the Major Basic Special Biological Resources Digital Development and Application Project in Yunnan Province (202002AA10007), the USDA National Institute of Food and Agriculture (1012359), and “111” Project (D21027).

Conflicts of Interest: The authors declare that they have no known competing financial interests or personal relationships that could have appeared to influence the work reported in this paper.

References

1. Wang, P. Y., Li, D. Z. (2019). *Dendrocalamus menghanensis* (Poaceae, Bambusoideae), a new woody bamboo from Yunnan, China. *PhytoKeys*, 130, 143–150. <https://doi.org/10.3897/phytokeys.130.33948>
2. Emamverdian, A., Ding, Y., Ranaei, F., Ahmad, Z. (2020). Application of bamboo plants in nine aspects. *The Scientific World Journal*, 2020, 7284203. <https://doi.org/10.1155/2020/7284203>
3. Wi, S. G., Lee, D. S., Nguyen, Q. A., Bae, H. J. (2017). Evaluation of biomass quality in short-rotation bamboo (*Phyllostachys pubescens*) for bioenergy products. *Biotechnology for Biofuels*, 10(1), 1–11. <https://doi.org/10.1186/s13068-017-0818-9>
4. Kokta, B. V., Ahmed, A. (1992). Feasibility of explosion pulping of bagasse. *Cellulose Chemistry and Technology*, 26(1), 107–123. <https://doi.org/10.1016/j.carbpol.2017.06.123>
5. Jeoh, T., Agblevor, F. A. (2001). Characterization and fermentation of steam exploded cotton gin waste. *Biomass and Bioenergy*, 21(2), 109–120. [https://doi.org/10.1016/s0961-9534\(01\)00028-9](https://doi.org/10.1016/s0961-9534(01)00028-9)
6. Lou, Z., Wang, Q., Kara, U. I., Mamtani, R. S., Zhou, X. et al. (2022). Biomass-derived carbon heterostructures enable environmentally adaptive wideband electromagnetic wave absorbers. *Nano-Micro Letters*, 14, 11. <https://doi.org/10.1007/s40820-021-00750-z>
7. Zhang, K., Wang, F., Liang, W., Wang, Z., Duan, Z. et al. (2018). Thermal and mechanical properties of bamboo fiber reinforced epoxy composites. *Polymers*, 10(6), 608. <https://doi.org/10.3390/polym10060608>
8. Gupta, A. (2020). Improvement of physiochemical properties of short bamboo fiber-reinforced composites using ceramic fillers. *Journal of Natural Fibers*, 17(11), 1582–1593. <https://doi.org/10.1080/15440478.2019.1584079>
9. Habibi, M. K., Lu, Y. (2014). Crack propagation in bamboo's hierarchical cellular structure. *Scientific Reports*, 4(1), 1–7. <https://doi.org/10.1038/srep05598>
10. Zequine, C., Ranaweera, C. K., Wang, Z., Singh, S., Tripathi, P. et al. (2016). High performance and flexible supercapacitors based on carbonized bamboo fibers for wide temperature applications. *Scientific Reports*, 6(1), 1–10. <https://doi.org/10.1038/srep31704>
11. Zhang, Q., Zeng, Y., Xiao, X., Deng, P., He, Q. et al. (2019). Investigation on the preparation and adsorption performance of bamboo fiber based activated carbon. *Fibers and Polymers*, 20(2), 293–301. <https://doi.org/10.1007/s12221-019-8336-y>
12. Jacquet, N., Maniet, G., Vanderghem, C., Delvigne, F., Richel, A. (2015). Application of steam explosion as pretreatment on lignocellulosic material: A review. *Industrial & Engineering Chemistry Research*, 54(10), 2593–2598. <https://doi.org/10.1021/ie503151g>
13. Karakoti, A., Biswas, S., Aseer, J. R., Sindhu, N., Sanjay, M. R. (2018). Characterization of microfiber isolated from *Hibiscus sabdariffa* var. *altissima* fiber by steam explosion. *Journal of Natural Fibers*, 17(2), 189–198. <https://doi.org/10.1080/15440478.2018.1477085>
14. Boonterm, M., Sunyadeth, S., Dedpakdee, S., Athichalinthorn, P., Patcharaphun, S. et al. (2016). Characterization and comparison of cellulose fiber extraction from rice straw by chemical treatment and thermal steam explosion. *Journal of Cleaner Production*, 134, 592–599. <https://doi.org/10.1016/j.jclepro.2015.09.084>
15. Tanpichai, S., Witayakran, S., Boonmahitthisud, A. (2019). Study on structural and thermal properties of cellulose microfibrils isolated from pineapple leaves using steam explosion. *Journal of Environmental Chemical Engineering*, 7(1), 102836. <https://doi.org/10.1016/j.jece.2018.102836>
16. Chen, G., Fang, C., Ran, C., Tan, Y., Yu, Q. et al. (2019). Comparison of different extraction methods for polysaccharides from bamboo shoots (*Chimonobambusa quadrangularis*) processing by-products. *International Journal of Biological Macromolecules*, 130, 903–914. <https://doi.org/10.1016/j.ijbiomac.2019.03.038>
17. Li, S., Yang, S., Shang, L., Liu, X., Ma, J. et al. (2021). 3D visualization of bamboo node's vascular bundle. *Forests*, 12(12), 1799. <https://doi.org/10.3390/fl2121799>

18. Lou, Z., Wang, Q., Sun, W., Liu, J., Yan, H. et al. (2022). Regulating lignin content to obtain excellent bamboo-derived electromagnetic wave absorber with thermal stability. *Chemical Engineering Journal*, 430(4), 133178. <https://doi.org/10.1016/j.ccej.2021.133178>
19. Rocky, B. P., Thompson, A. J. (2018). Production of natural bamboo fibers-3: SEM and EDX analyses of structures and properties. *AATCC Journal of Research*, 5(6), 27–35. <https://doi.org/10.14504/ajr.5.6.4>
20. Baral, N. R., Shah, A. (2017). Comparative techno-economic analysis of steam explosion, dilute sulfuric acid, ammonia fiber explosion and biological pretreatments of corn stover. *Bioresource Technology*, 232, 331–343. <https://doi.org/10.1016/j.biortech.2017.02.068>
21. Phinichka, N., Kaenthong, S. (2018). Regenerated cellulose from high alpha cellulose pulp of steam-exploded sugarcane bagasse. *Journal of Materials Research and Technology*, 7(1), 55–65. <https://doi.org/10.1016/j.jmrt.2017.04.003>
22. Maache-Rezzoug, Z., Pierre, G., Nouviaire, A., Maugard, T., Rezzoug, S. A. (2011). Optimizing thermomechanical pretreatment conditions to enhance enzymatic hydrolysis of wheat straw by response surface methodology. *Biomass and Bioenergy*, 35(7), 3129–3138. <https://doi.org/10.1016/j.biombioe.2011.04.012>
23. Khawas, P., Deka, S. C. (2016). Isolation and characterization of cellulose nanofibers from culinary banana peel using high-intensity ultrasonication combined with chemical treatment. *Carbohydrate Polymers*, 137, 608–616. <https://doi.org/10.1016/j.carbpol.2015.11.020>
24. Chen, C., Li, Z., Mi, R., Dai, J., Xie, H. et al. (2020). Rapid processing of whole bamboo with exposed, aligned nanofibrils toward a high-performance structural material. *ACS Nano*, 14(5), 5194–5202. <https://doi.org/10.1021/acsnano.9b08747.s001>
25. Cheng, D., Jiang, S., Zhang, Q. (2013). Effect of hydrothermal treatment with different aqueous solutions on the mold resistance of moso bamboo with chemical and FTIR analysis. *BioResources*, 8(1), 371–382. <https://doi.org/10.15376/biores.8.1.371-382>
26. Xu, K., Li, Q., Xie, L., Shi, Z., Su, G. et al. (2022). Novel flexible, strong, thermal-stable, and high-barrier switchgrass-based lignin-containing cellulose nanofibrils/chitosan biocomposites for food packaging. *Industrial Crops and Products*, 179, 114661. <https://doi.org/10.1016/j.indcrop.2022.114661>
27. Sui, W., Chen, H. (2016). Effects of water states on steam explosion of lignocellulosic biomass. *Bioresource Technology*, 199, 155–163. <https://doi.org/10.1016/j.biortech.2015.09.001>
28. Chen, H., Li, G., Li, H. (2014). Novel pretreatment of steam explosion associated with ammonium chloride preimpregnation. *Bioresource Technology*, 153, 154–159. <https://doi.org/10.1016/j.biortech.2013.11.025>
29. Chen, W., Zhang, S., Li, Y., Wu, H., Meng, Q. et al. (2019). Steam-exploded sugarcane bagasse as a potential beef cattle feedstock: Effects of different pretreatment conditions. *Journal of Animal Science*, 97(6), 2414–2423. <https://doi.org/10.1093/jas/skz127>
30. Daniloski, D., McCarthy, N. A., O’Callaghan, T. F., Vasiljevic, T. (2022). Authentication of β -casein milk phenotypes using FTIR spectroscopy. *International Dairy Journal*, 129, 105350. <https://doi.org/10.1016/j.idairyj.2022.105350>
31. Zhou, Y., Niu, S., Li, J. (2016). Activity of the carbon-based heterogeneous acid catalyst derived from bamboo in esterification of oleic acid with ethanol. *Energy Conversion and Management*, 114, 188–196. <https://doi.org/10.1016/j.enconman.2016.02.027>
32. Liang, F., Wang, R., Hongzhong, X., Yang, X., Zhang, T. et al. (2018). Investigating pyrolysis characteristics of moso bamboo through TG-FTIR and Py-GC/MS. *Bioresource Technology*, 256, 53–60. <https://doi.org/10.1016/j.biortech.2018.01.140>
33. Tanpichai, S., Biswas, S. K., Witayakran, S., Yano, H. (2019). Water hyacinth: A sustainable lignin-poor cellulose source for the production of cellulose nanofibers. *ACS Sustainable Chemistry & Engineering*, 7(23), 18884–18893. <https://doi.org/10.1021/acssuschemeng.9b04095>
34. Stefanidis, S. D., Kalogiannis, K. G., Iliopoulou, E. F., Michailof, C. M., Pilavachi, P. A. et al. (2014). A study of lignocellulosic biomass pyrolysis via the pyrolysis of cellulose, hemicellulose and lignin. *Journal of Analytical and Applied Pyrolysis*, 105, 143–150. <https://doi.org/10.1016/j.jaap.2013.10.013>
35. Xue, Q., Peng, W., Ohkoshi, M. (2014). Molecular bonding characteristics of self-plasticized bamboo composites. *Pakistan Journal of Pharmaceutical Sciences*, 27(4). https://doi.org/10.1007/978-981-15-8489-3_12

36. Liu, Z., Fei, B., Jiang, Z., Cai, Z., Yu, Y. et al. (2013). A comparative study of thermal properties of sinocalamus affinis and moso bamboo. *Journal of Thermal Analysis and Calorimetry*, 111(1), 393–399. <https://doi.org/10.1007/s10973-012-2266-x>
37. Reis, R. S., Tienne, L. G., de H. S. Souza, D., Maria de Fátima, V. M., Monteiro, S. N. (2020). Characterization of coffee parchment and innovative steam explosion treatment to obtain microfibrillated cellulose as potential composite reinforcement. *Journal of Materials Research and Technology*, 9(4), 9412–9421. <https://doi.org/10.1016/j.jmrt.2020.05.099>
38. Yun, H., Li, K., Tu, D., Hu, C. (2016). Effect of heat treatment on bamboo fiber morphology crystallinity and mechanical properties. *Wood Research*, 61(2), 227–234. <https://doi.org/10.17702/jai.2016.17.3.96>
39. Han, G., Deng, J., Zhang, S., Bicho, P., Wu, Q. (2010). Effect of steam explosion treatment on characteristics of wheat straw. *Industrial Crops and Products*, 31(1), 28–33. <https://doi.org/10.1016/j.indcrop.2009.08.003>
40. Xu, K., Liu, C., Kang, K., Zheng, Z., Wang, S. et al. (2018). Isolation of nanocrystalline cellulose from rice straw and preparation of its biocomposites with chitosan: Physicochemical characterization and evaluation of interfacial compatibility. *Composites Science and Technology*, 154, 8–17. <https://doi.org/10.1016/j.compscitech.2017.10.022>
41. Sharma, B., Shah, D. U., Beaugrand, J., Janeček, E. R., Scherman, O. A. et al. (2018). Chemical composition of processed bamboo for structural applications. *Cellulose*, 25, 3255–3266. <https://doi.org/10.1007/s10570-018-1789-0>
42. Wang, W., Guo, T., Sun, K., Jin, Y., Gu, F. et al. (2019). Lignin redistribution for enhancing barrier properties of cellulose-based materials. *Polymers*, 11(12), 1929. <https://doi.org/10.3390/polym11121929>
43. Chen, Q., Zhang, R., Wang, Y., Wen, X., Qin, D. (2016). The effect of bamboo charcoal on water absorption, contact angle, and the physical-mechanical properties of bamboo/low-density polyethylene composites. *BioResources*, 11(4), 9986–10001. <https://doi.org/10.15376/biores.11.4.9986-10001>
44. Li, C., Sun, Y., Zhang, L., Li, Q., Zhang, S. et al. (2022). Sequential pyrolysis of coal and biomass: Influence of coal-derived volatiles on property of biochar. *Applications in Energy and Combustion Science*, 9, 100052. <https://doi.org/10.1016/j.jaeacs.2021.100052>
45. Xu, J., Chen, Y., Cheng, J. J., Sharma-Shivappa, R., Burns, J. (2011). Delignification of switchgrass cultivars for bioethanol production. *BioResources*, 6(1), 707–720. <https://doi.org/10.15376/biores.6.1.707-720>
46. Wang, X., Cheng, K. J. (2020). Effect of glow-discharge plasma treatment on contact angle and micromorphology of bamboo green surface. *Forests*, 11(12), 1293. <https://doi.org/10.3390/f11121293>
47. Kim, S. H., Yeon, Y. K., Lee, J. M., Chao, J. R., Lee, Y. J. et al. (2018). Precisely printable and biocompatible silk fibroin bioink for digital light processing 3D printing. *Nature Communications*, 9(1), 1–14. <https://doi.org/10.1038/s41467-018-03759-y>
48. Zhang, Y. C., Wu, H. Y., Qiu, Y. P. (2010). Morphology and properties of hybrid composites based on polypropylene/poly(lactic acid) blend and bamboo fiber. *Bioresource Technology*, 101(20), 7944–7950. <https://doi.org/10.1016/j.biortech.2010.05.007>
49. Li, Y., Jiang, L., Xiong, C., Peng, W. (2015). Effect of different surface treatment for bamboo fiber on the crystallization behavior and mechanical property of bamboo fiber/nanohydroxyapatite/poly(lactic-co-glycolic) composite. *Industrial & Engineering Chemistry Research*, 54(48), 12017–12024. <https://doi.org/10.1021/acs.iecr.5b02724>
50. Yu, Y., Wang, H., Lu, F., Tian, G., Lin, J. (2014). Bamboo fibers for composite applications: A mechanical and morphological investigation. *Journal of Materials Science*, 49, 2559–2566. <https://doi.org/10.1007/s10853-013-7951-z>